Memorias del XX Congreso Latinoamericano de Control Automático (CLCA 2025)
13-17 de Octubre, 2025. Cancún, Quintana Roo, México

Extended state observers in consensus: application to slope compensation in cruise control algorithms

Alejandra de la Guerra * **J. F. Guerrero-Castellanos** **

* *Universidad de las Américas Puebla, Ex-Hacienda Santa Catarina Mártir, 72810, San Andrés Cholula, Puebla, México (e-mail:alejandra.delaguerra@udlap.mx)*
** *Benemérita Universidad Autónoma de Puebla (BUAP), Facultad de Ciencias de la Electrónica, Puebla, México(e-mail:fermi.guerrero@correo.buap.mx)*

Abstract: This paper presents a cruise control with road condition compensation based on discrete extended state observers. The road condition compensator operates as a multi-agent systems in consensus to achieve real-time disturbance estimation under measurement noise. The road characteristics considered in this study include the friction coefficient and slope. Numerical simulations are provided to validate the proposed road condition compensation scheme for four different slope angles with measurement noise for two types of graphs: ring and star.

Keywords: Observers, multi-agents, disturbance estimation.

1. INTRODUCTION

Active vehicle control systems are an ongoing subject of research across many fields. These systems improve driving performance, stability, and comfort by adjusting parameters such as suspension, steering, and braking in real time. Using sensors, actuators, and control algorithms, their goal is to enhance both safety and performance. Representative examples include active suspension, stability control (yaw or rollover), and active steering systems.

The design of such control laws often requires knowledge of road conditions to remain robust against environmental changes. Another motivation for identifying or compensating road characteristics is cost reduction, by eliminating the need for expensive sensors. Furthermore, accurate estimation of road conditions is essential for the realization of fully autonomous driving (Khan et al., 2022).

Two main road characteristics are considered in this work: the road friction coefficient and the road slope. Recent studies include Xia et al. (2019), who used a least-squares forgetting factor method to identify vehicle resistance forces, including slope, validated through simulations of a full vehicle dynamics model. Yue et al. (2024) applied a least-squares approach to identify slope and vehicle mass to optimize automatic transmission performance, verified by hardware-in-the-loop testing. Yong et al. (2019) combined an IMM-Kalman filter with a lookup table to identify friction coefficients and variable slopes, also validated via hardware-in-the-loop experiments. Hao et al. (2017) employed a Kalman filter to estimate slope gradient and vehicle mass using acceleration measurements, validated through simulations and inertial navigation data. Guo et al. (2022) proposed slope estimation based on a Sage–Husa adaptive Kalman filter, tested with real-vehicle data.

Regarding disturbance compensation using multi-agent consensus, Ding (2015) proposed a disturbance observer relying on relative state information, where observer gains depended on network connectivity, validated in flight formation simulations. Sun et al. (2018) investigated consensus-based disturbance rejection for linear multi-agent systems using relative state data with both state and disturbance observers. Li et al. (2020) designed a variable-based observer with an adaptive law for partial fault detection, evaluated through numerical simulation.

In this work, we propose an online compensation method for road friction and slope. Considering that active control systems must be implemented on microcontrollers, a discrete-time implementation is required for practical deployment as in Vásquez Cruz et al. (2024). We therefore implement a multi-agent system using discrete extended state observer (ESO). Multiple ESOs operate simultaneously, forming a multi-agent network to estimate the slope value. A consensus law corrects disturbance estimation,

[1] This paper is partially funded by the Vicerrectoría de Investigación y Estudios de Posgrado (VIEP-BUAP) under grant number 00593-PV/2025.

https://doi.org/10.58571/CNCA.AMCA.2025.071

and the resulting speed estimates are used to compensate disturbance effects in the speed control loop. As far as the authors know, there are no similar works in the literature.

The paper is organized as follows: Section 2 presents the preliminaries and the statement problem; Section 3 defines the collaborative extended state observers used in this work; Section 4 introduces the road condition compensation design; Section 5 includes the numerical simulations used to validate the cruise control algorithm. Finally, Section 6 presents the work conclusions.

2. PRELIMINARIES AND STATEMENT PROBLEM

2.1 Graph Theory

Consider a graph $\mathcal{G} = \{\mathcal{V}, \mathcal{E}\}$ consisting of a set of vertices (or nodes) $\mathcal{V} = 1, \ldots, N$ and edges $\mathcal{E} \in \mathcal{V} \times \mathcal{V}$. If there is an edge (i, j) between nodes i and j, with $1 \leq i \leq N$ and $1 \leq j \leq N$, then i and j are called adjacent, i.e. $\mathcal{E} = (i, j) \in \mathcal{V} \times \mathcal{V} : i, j$ *adjacent*. An entry of the adjacency matrix $\mathcal{A}$ is defined by $a_{ij} = 1$ if i and j are adjacent and $a_{ij} = 0$ otherwise. Note that the diagonal elements of the adjacency matrix are all zero for a graph without any loop (as in the present paper). $\mathcal{G}$ is called undirected if $(i, j) \in \mathcal{E} \Leftrightarrow (j, i) \in \mathcal{E}$. A path from i to j is a sequence of distinct nodes, starting from i and ending with j, such that each pair of consecutive nodes is adjacent. If there is a path from i to j, then i and j are called connected. If all pairs of nodes in $\mathcal{G}$ are connected, then $\mathcal{G}$ is called connected. The distance $d(i, j)$ between two nodes is the number of edges of the shortest path from i to j. The diameter $\mathbf{d}$ of $\mathcal{G}$ is the maximum distance $d(i, j)$ over all pairs of nodes. The degree (or valency) matrix $\mathbf{D}(\mathcal{G})$ of $\mathcal{G}$ is a diagonal matrix whose diagonal elements d_i are equal to the cardinality of node i's neighbor set $\mathcal{N}_i = \{j \in \mathcal{V} : (i, j) \in \mathcal{E}\}$. The Laplacian matrix $\mathcal{L}$ of $\mathcal{G}$ is defined as $\mathcal{L} = \mathbf{D}(\mathcal{G}) - \mathcal{A}(\mathcal{G})$. For undirected graphs, $\mathcal{L}$ is symmetric and positive semi-definite, i.e. $\mathcal{L} = \mathcal{L}^T \geq 0$. The row sums of $\mathcal{L}$ are zero. Thus, the vector of ones $\mathbf{1}$ is an eigenvector corresponding to eigenvalue $\lambda_i(\mathcal{G}) = 0$, i.e. $\mathcal{L} \cdot \mathbf{1} = 0$.

2.2 Statement problem

Let us consider the following class of non-linear systems

$$\Sigma_{\text{NL}} : \begin{cases} \dot{\mathbf{x}}(t) = \mathbf{A}\mathbf{x}(t) + \mathbf{B}u(t) + \mathbf{E}\xi(\mathbf{x}(t), d(t)) \\ \mathbf{y}_i(k) = \mathbf{C}\mathbf{x}(k), \end{cases} \tag{1}$$

where $\mathbf{x}(t) \in \mathbb{R}^n$ is the state of the system, $u(t) \in \mathbb{R}$ is the control action, $\xi(\mathbf{x}(t), d(t))) : \mathbb{R}^n \times \mathbb{R} \to \mathbb{R}$ is a signal that lumps external disturbances and mismatches between the real plant and the model, and $\mathbf{y}_i(k) \in \mathbb{R}^{n_y}$ is a discrete measurable output obtained through the *i-th* sensor with $i \in \{1, 2...N\}$. In order to develop a collaborative observer, one rewrites (1) in a discretized extended-state form, considering $\xi(\cdot)$ a piecewise constant function:

$$\Sigma_{\text{NLD}} : \begin{cases} \mathbf{x}(k+1) = \mathbf{A_d}\mathbf{x}(k) + \mathbf{B}_{\text{d}}u(t) + \mathbf{E}_{\text{d}}\xi(\mathbf{x}(k), d(k)) \\ \xi(k+1) = \xi(k) \\ \mathbf{y}_i(k) = \mathbf{C}\mathbf{x}(k), \end{cases} \tag{2}$$

with

$$\boldsymbol{A_d} = e^{\boldsymbol{A}T_s}, \quad \boldsymbol{B_d} = \int_0^{T_s} e^{\boldsymbol{A}\theta} d\theta \boldsymbol{B}, \quad \boldsymbol{E_d} = \int_0^{T_s} e^{\boldsymbol{A}\theta} d\theta \boldsymbol{E}.$$

The aim is to estimate $\mathbf{x}(k)$ and $\xi(k)$ in terms of N available noisy measurements $\mathbf{y}_i(k)$ obtained through a group of sensors. Each sensor and its corresponding algorithm are considered a node, which exchanges information with other nodes to collectively reach an estimate of the underlying state and disturbance. Then, the estimate are employed to compute a control action.

3. COLLABORATIVE ESO

A multi-agent system consists of multiple control units or agents that work together, sharing information, to achieve a common objective such as consensus, formation control, or distributed optimization. In this work various extended state observers will be the agents, each one will contribute with its disturbance estimate to reach a disturbance estimation consensus.
To accomplish this task, one can use the Proportional Integral Observer (PIO) structure, representing a discretized version of the generalized ESO. However, in these observers, the estimated state is predicted a step ahead. This is why these observers are known as predictive observers (Franklin et al., 1990). This means that the estimated state at the instant k depends on measurements made at the instant $k-1$, although $\mathbf{y}(k)$ might already be available. Then, a current observer is considered, which allows the incorporation of the most recent measurement into the current estimate. It is carried out by splitting the estimation into two steps, prediction, and correction.

$$\Sigma_{\text{Obs}} : \begin{cases} \hat{\mathbf{z}}_i^-(k) = \tilde{\mathbf{A}}_{\text{d}}\hat{\mathbf{z}}_i(k-1) + \tilde{\mathbf{B}}_{\text{d}}u(k-1) \\ \hat{\mathbf{z}}_{\mathbf{i}}(k) = \hat{\mathbf{z}}_{\mathbf{i}}^-(k) + \mathbf{L}(\mathbf{y}_i(k) - \tilde{\mathbf{C}}\mathbf{z}_i^-(k)) \\ \qquad + \sum_{j \in N_i} k_c(\hat{\mathbf{z}}_j^-(k) - \hat{\mathbf{z}}_i^-(k)) \end{cases} \tag{3}$$

where

$$\hat{\mathbf{z}}_i(k) = \begin{pmatrix} \hat{\mathbf{x}}_i(k) \\ \hat{\xi}_i(k) \end{pmatrix}; \ \tilde{\mathbf{A}}_{\text{d}} = \begin{pmatrix} \mathbf{A}_{\text{d}} & \mathbf{E}_{\text{d}} \\ \mathbf{0} & 1 \end{pmatrix} \tag{4}$$

$$\tilde{\mathbf{B}}_{\text{d}} = \begin{pmatrix} \mathbf{B}_{\text{d}} \\ \mathbf{0} \end{pmatrix}; \ \tilde{\mathbf{C}} = \begin{pmatrix} \mathbf{C} & \mathbf{0} \end{pmatrix} \tag{5}$$

Assumption 1. Let's consider the first part of (3), that is,

$$\Sigma_{\text{Obs}} : \begin{cases} \hat{\mathbf{z}}_i^-(k) = \tilde{\mathbf{A}}_{\text{d}}\hat{\mathbf{z}}_i(k-1) + \tilde{\mathbf{B}}_{\text{d}}u(k-1) \\ \hat{\mathbf{z}}_{\mathbf{i}}(k) = \hat{\mathbf{z}}_{\mathbf{i}}^-(k) + \mathbf{L}(\mathbf{y}_i(k) - \tilde{\mathbf{C}}\mathbf{z}_i^-(k)) \end{cases} \tag{6}$$

 https://doi.org/10.58571/CNCA.AMCA.2025.071

then let's assume that the vector $\mathbf{L}$ is choosing such that $|\lambda_l(\mathbf{A}_\mathrm{O})| < 1$, being $\lambda_l(\mathbf{A}_\mathrm{O})$ the eigenvalues of $\mathbf{A}_\mathrm{O} = \left(\tilde{\mathbf{A}}_\mathrm{d} - \mathbf{L}\tilde{\mathbf{C}}\tilde{\mathbf{A}}_\mathrm{d}\right)$ and $l \in \{1, \cdots, n+1\}$. Then the error vector defined as $\tilde{\mathbf{z}}^- := \mathbf{z} - \hat{\mathbf{z}}^- \to 0$ as $k \to \infty$.

Now we are ready to declare our main result.

Proposition 1. Consider a sensor network with N sensors and topology $\mathcal{G} = \{\mathcal{V}, \mathcal{E}\}$, that is a connected graph observing a process (2) using the sensor measurements $\mathbf{y}_i(k)$. Assume that $\mathbf{A}_d$ and $\mathbf{C}$ are observable and assume the nodes of the network implement the observer (3). Then, the distributive observers solve the consensus problems that allow them to calculate the average of the state $\hat{\mathbf{z}}_i(k)$ and $\hat{\mathbf{x}}(k) \to \mathbf{x}(k)$ and $\hat{\xi}(k) \to \xi(k)$ when $k \to \infty$.

Proof 1. Consider the correction stage of the observer (3),

$$\Sigma_{\mathrm{Obs}} : \begin{cases} \hat{\mathbf{z}}_\mathbf{i}(k) = \hat{\mathbf{z}}_\mathbf{i}^-(k) + \mathbf{L}(\mathbf{y}_i(k) - \tilde{\mathbf{C}}\mathbf{z}_i^-(k)) \\ \qquad + \sum_{j \in N_i} k_c(\hat{\mathbf{z}}_j^-(k) - \hat{\mathbf{z}}_i^-(k)) \end{cases} \tag{7}$$

and let us define the following vectors:
$\hat{\mathbf{Z}}(k) = (\hat{\mathbf{z}}_1(k), \hat{\mathbf{z}}_2(k)), \cdots, \hat{\mathbf{z}}_N(k))^T$
$\hat{\mathbf{Z}}^-(k) = (\hat{\mathbf{z}}_1^-(k), \hat{\mathbf{z}}_2^-(k)), \cdots, \hat{\mathbf{z}}_N^-(k))^T$
$\mathbf{Z}^(k) = (\mathbf{z}_1(k), \mathbf{z}_2(k), \cdots, \mathbf{z}_N(k))^T$
where

$$\mathbf{z}_i(k) = \begin{pmatrix} \mathbf{x}_i(k) \\ \xi_i(k) \end{pmatrix} \tag{8}$$

In matrix form (for all the nodes) (7) can be rewritten as

$$\hat{\mathbf{Z}}(k) = \mathbf{W}\hat{\mathbf{Z}}^-(k) + \mathbf{L}\tilde{\mathbf{C}}(\mathbf{Z}(k) - \hat{\mathbf{Z}}^-(\mathbf{k})) \tag{9}$$

where

$$\mathbf{W} = \mathbf{I} - k_c\mathcal{L} \tag{10}$$

with $\mathcal{L}$ the Laplacian of the topology $\mathcal{G}$. Since one considers connected undirected graphs, and choosing k_c such that $0 < k_c < \frac{2}{\lambda_{\max_{i\geq 2}}(\mathcal{L})}$, the eigenvalues of $\mathbf{W}$ satisfy

$$1 = \lambda_1(\mathbf{W}) > \max_{i \geq 2} |\lambda_i(\mathbf{W})| =: \alpha < 1.$$

That is, $\mathbf{W}$ restricted to the orthogonal subspace $\{\mathbf{1}\}^\perp$ has spectral radius $\alpha < 1$. Unrolling (9) and by Assumption 1, it gives

$$\hat{\mathbf{Z}}(k) = \frac{1}{N}\sum_{i=1}^{N} \hat{\mathbf{Z}}^-(k) \tag{11}$$

4. ROAD CONDITION COMPENSATOR

The road condition compensator is comprised by a collaborative ESO and a speed PI control. Its objective it to compensate the effect of the road slope variation in low speed with an uniform performance in a speed interval of operation. Next, the kinetic model of a vehicle is recalled from Husain (2021).

4.1 Kinetic model of a vehicle

It is assumed that a vehicle moves on a road in a tangential direction in a forward motion with unknown slope changes. A tangential co-ordinate system is attached to the center of gravity of the vehicle (cg). The tangential systems origin is aligned with a fixed co-ordinate system where both systems shared the same z direction but the x and y directions of the tangential system will change with the slope in the roadway. Using Newton's second law in the cg, the vehicle's motion in the tangential co-ordinate system can be modeled as

$$\sum F_T = m\frac{dv_T}{dt}\,, \tag{12}$$

where m is the vehicle total mass. Given that the gravitational force is compensate by road reaction force, there is not motion in the y_T direction. it is assumed that there is not motion in the z_T direction either. Thus, the total contribution of motion is in the x_T direction with velocity given by v_{xT}. The propulsion unit will produce the tractive force F_{TR} to move the vehicle forward. The sum of opposing forces are defined as the road load, F_{RL}. In this work these opposing forces will be represented by a viscous friction term and the force term related to the gravitational force, F_{gxT}, expressed as

$$F_{RL} = bv_{xt} + F_{gxT}\,, \tag{13}$$

where b is the viscous friction coefficient. On the other hand, the gravitational force depends on the slope of the road. This force will be positive when mounting a slope and negative when descending it. The gravitational force is defined as

$$F_{gxT} = mg\sin(\beta)\,, \tag{14}$$

with g the gravitational acceleration constant and β is the slope angle. Therefore, substituting equations (13-14) in equation (12), the vehicle's motion can be modeled by the expression

$$\frac{dv_{xT}}{dt} = -\frac{b}{m}v_{xT} + g\sin(\beta) + \frac{1}{m}F_{TR}\,. \tag{15}$$

For a more detailed description of some of the main opposing forces and a description of the vehicle's dynamical model, the book by Husain (2021) is highly recommended.

Note that (15) belongs to the class of non-linear systems described by (1), with $\xi(\cdot) = g\sin(\beta)$. Then, it admits a discretized extended-state form, considering $\xi(\cdot)$ a piecewise constant function, similar to (2)

4.2 Observer and control

The state space equations for model (15) can be written as

$$\dot{\boldsymbol{x}}(t) = \begin{bmatrix} 0 & 1 \\ 0 & -\frac{b}{m} \end{bmatrix}\boldsymbol{x}(t) + \begin{bmatrix} 0 \\ \frac{1}{m} \end{bmatrix}F_{TR}(t) + \begin{bmatrix} 0 \\ 1 \end{bmatrix}\xi\,, \tag{16}$$

$$y(t) = \begin{bmatrix} 1 & 0 \end{bmatrix}\boldsymbol{x}(t)\,, \tag{17}$$

 https://doi.org/10.58571/CNCA.AMCA.2025.071

with $\xi = g\sin(\beta)$. Model (16-17) in discrete time, using a ZOH with $T_s = 2\,[s]$, can be expressed as

$$\boldsymbol{x}_{k+1} = \begin{bmatrix} 1 & 1.951 \\ 0 & 0.9515 \end{bmatrix} \boldsymbol{x}_k + \begin{bmatrix} 0.002843 \\ 0.00282 \end{bmatrix} u_k + \begin{bmatrix} 1.9673 \\ 1.9511 \end{bmatrix} \xi_k \,. \tag{18}$$

$$y(k) = \begin{bmatrix} 1 & 0 \end{bmatrix} \boldsymbol{x}(k) \,. \tag{19}$$

Assuming that the output $y(k)$ can be measured by i sensors, there would be $y_i(k)$ outputs available. Then, the current observer for the $i-$th measurement can be written as in equations (3-5). Gains of vector $\boldsymbol{L}_c$ can be defined by assigning the characteristic equation poles inside the unitary circle in the z plane,

$$det(z\boldsymbol{I} - (\boldsymbol{\Phi} - \boldsymbol{L}_c\boldsymbol{C}\boldsymbol{\Phi})) = (z - z_d)^3 \,. \tag{20}$$

Moreover, the continuous time observer poles and the discrete time observer poles are related by the next equation

$$z_d = exp(-\omega_0 T_s/\epsilon) \,.$$

Finally, the next matrix definition are included to complete the observer implementation.

$$\boldsymbol{\Phi} = \begin{bmatrix} 1 & T_s & T_s^2/2 \\ 0 & 1 & T_s \\ 0 & 0 & 1 \end{bmatrix} ,$$

$$\boldsymbol{\Gamma} = b \begin{bmatrix} T_s^2/2 \\ T_s \\ 0 \end{bmatrix} ,$$

$$\boldsymbol{C} = \begin{bmatrix} 1 & 0 & 0 \end{bmatrix} ,$$

$$\boldsymbol{L}_c = \begin{bmatrix} 1 - z_d^3 \\ \frac{3}{2T_s}(1 - z_d)^2(1 + z_d) \\ \frac{1}{T_s}(1 - z_d)^3 \end{bmatrix} ,$$

On the other hand, the controller is a PI with a disturbance rejection term described by the expressions

$$u(k) = K_p e(k) + K_i e(k-1) - B_d^+ E_d \hat{z}_2(k) \,, \tag{21}$$

with K_p and K_i the proportional and integral gains respectively, B_d^+ the pseudo inverse matrix of B_d, and $e(k) = y(k) - \hat{x}_2(k)$, $e(k-1) = y(k-1) - \hat{x}_2(k-1)$.

5. SIMULATION

The proposed road condition compensation scheme, based on the ESO observer, was evaluated using MATLAB. A light vehicle model with parameters from (Husain, 2021) was employed. The system parameters are summarized in Table 1.

Since realistic road slopes are typically below $\beta = 15°$, four slope disturbances were considered: $[0°, 5°, 10°, 15°]$. The reference velocity was set at 25[km/h] = 7[m/s], consistent with climbing scenarios.

Table 1. Vehicle parameters.

Parameter	**Value**
mass (m)	692 [kg]
friction coefficient (b)	17.1890 [Ns/m]
gravitational acceleration constant (g)	9.81 $[m/s^2]$

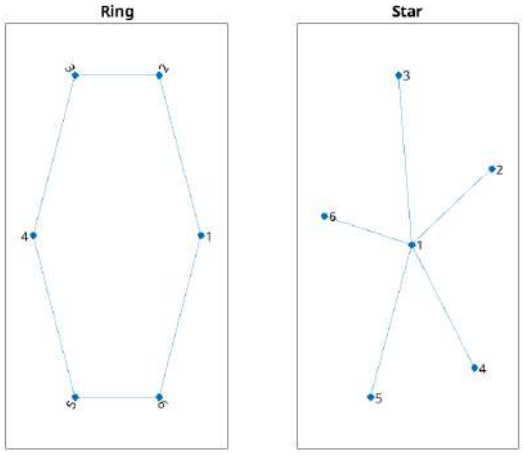

Fig. 1. Graph topologies used in the simulation, the estimated speed is taken from node 1 in both cases

Controller gains are calculated as $K_p = 2m\epsilon_0\omega$, $K_i = m\omega^2$ where $\epsilon_0 = 0.1$, $\omega_0 = 0.0248$, $\omega = 5\omega_0$. While for the four observes the tuning parameters where chosen has $\epsilon = 0.9, \omega_1 = 50\omega_0$, $T_s = 2\,[s]$, therefore $z_d = 0.636$, $L = [0.9997 \quad 0.6995 \quad 0.4384]^T$, the consensus gain $k = 0.6$. All simulations included output's white noise with $\sigma = 0.01$ standard deviation.

5.1 Graph

The simulations where made for two types of graphs: ring and star that can be seen in Figure 1. Star topologies use a central hub, connecting each device individually to it, while ring topologies connect each device to its two immediate neighbors, forming a closed loop. Key differences include star having a single point of failure (the hub or node one), and high resilience. Whereas, ring topologies have each node as a potential failure point, lower initial cost, less reliable and it's more difficult to add nodes.

5.2 Discussion

The results, show in Figure 2–5, demonstrate that the ESO-based consensus can estimate the states and the disturbance in the presence of noise. Also, Root Mean Square (RMS) error values for speed regulation and speed estimation estimations are presented in Tables 2 and 3. Key observations include:

 https://doi.org/10.58571/CNCA.AMCA.2025.071

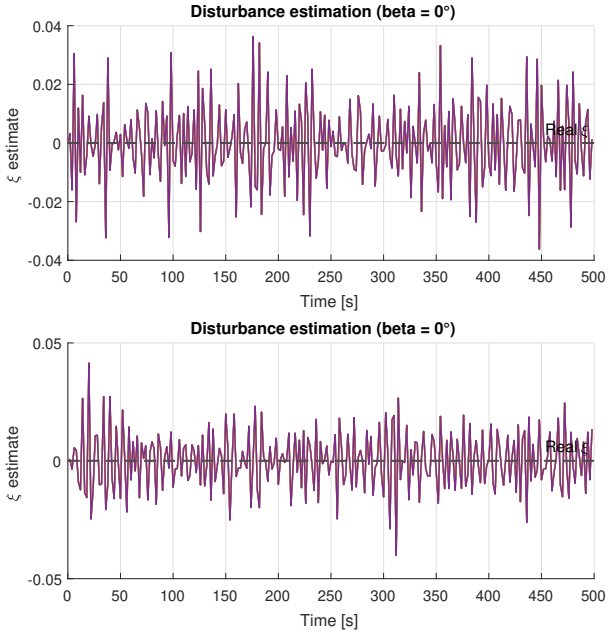

Fig. 2. Disturbance estimation observers consensus $\beta = 0°$. Upper: Ring. Lower: Star.

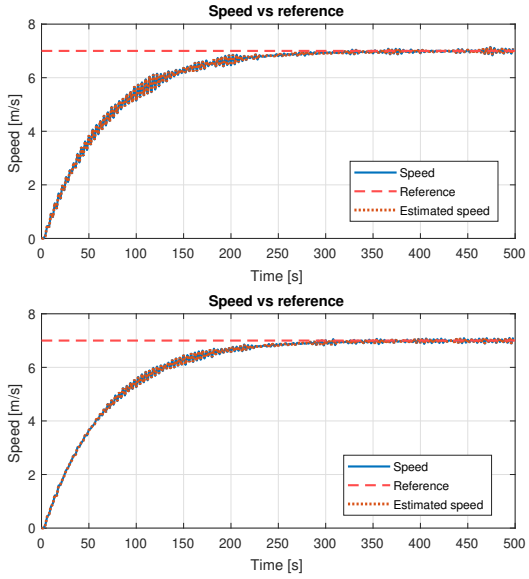

Fig. 3. Speed control and estimation $\beta = 0°$. Upper: Ring. Lower: Star.

- The scheme compensates slope effects on speed control with uniform performance across slope values.
- The RMS error values show that there is a minimal difference when using a ring or a star graph. However, their advantages and disadvantages are commonly known.
- Although simulations assumed multiple sensors, the scheme can also be implemented as digital twins with varying disturbance models.

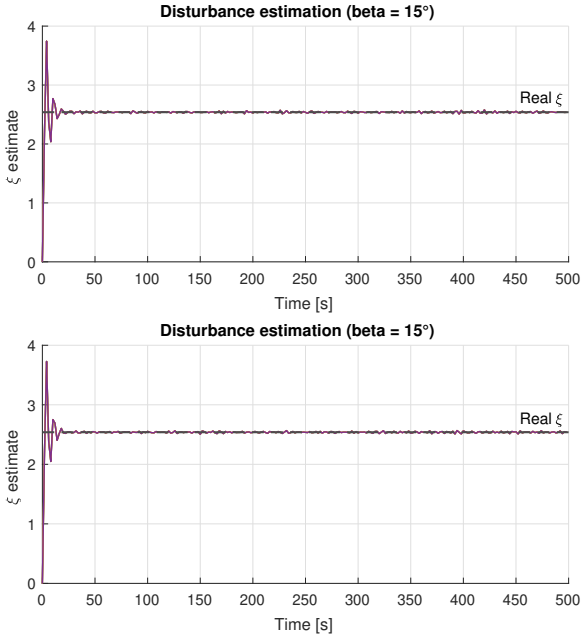

Fig. 4. Disturbance estimation observers consensus $\beta = 15°$. Upper: Ring. Lower: Star.

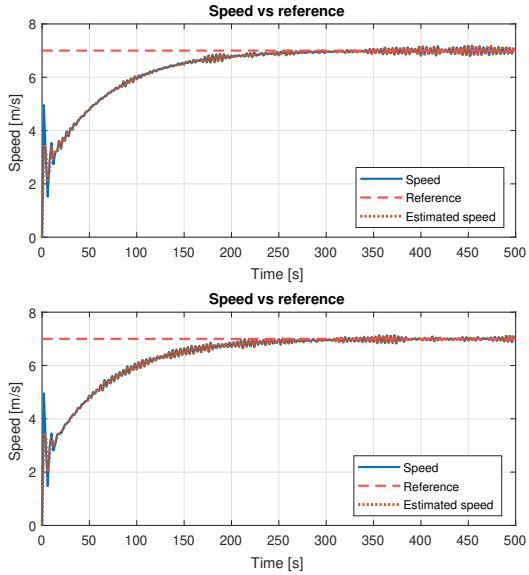

Fig. 5. Speed control and estimation $\beta = 15°$. Upper: Ring. Lower: Star.

- The system maintains uniform performance in the presence of sensor noise, with disturbance estimation and regulation speed largely unaffected for all the slope values. Uniform performance is key to guarantee comfort driving for all scenarios.

6. CONCLUSIONS

This work proposed a road condition compensation scheme based on consensus among extended state ob-

 https://doi.org/10.58571/CNCA.AMCA.2025.071

Table 2. Speed regulation error RMS value.

	e_{RMS}	
Angle/Graph	**RING**	**STAR**
$\beta = 0°$	1.8801	1.8821
$\beta = 5°$	1.6794	1.6663
$\beta = 10°$	1.4580	1.4569
$\beta = 15°$	1.2552	1.2554

Table 3. Speed estimation error RMS value.

	$\mathbb{E}_{RMS}$	
Angle/Graph	**RING**	**STAR**
$\beta = 0°$	0.0116	0.0113
$\beta = 5°$	0.0362	0.0353
$\beta = 10°$	0.0693	0.0716
$\beta = 15°$	0.1044	0.1063

servers. The approach effectively compensates for slope disturbances, ensuring uniform speed control performance even under sensor noise. This scheme may contribute to cost-effective active vehicle control systems by enable the use of simpler and low-cost sensors in multi agent consensus.

Future research will include experimental validation of the proposed framework, using different positions sensors with different noise values. Additionally, the estimation of parameters such as vehicle mass and friction coefficient will be explored. Another direction for future study is the coupling between road slope and vehicle body pitch, as discussed in Liu et al. (2023); Kim et al. (2018).

REFERENCES

Ding, Z. (2015). Consensus disturbance rejection with disturbance observers. *IEEE Transactions on Industrial Electronics*, 62(9), 5829–5837.

Franklin, G.F., Powell, J.D., and Workman, M.L. (1990). *Digital Control of Dynamic Systems*. Electrical and Computer Engineering; Control Engineering. Addison-Wesley, Reading Massachusetts, second edition. A SRL reference.

Guo, J., He, C., Li, J., and Wei, H. (2022). Slope estimation method of electric vehicles based on improved sage–husa adaptive kalman filter. *Energies*, 15(11), 4126.

Hao, S., Luo, P., and Xi, J. (2017). Estimation of vehicle mass and road slope based on steady-state kalman filter. In *2017 IEEE International Conference on Unmanned Systems (ICUS)*, 582–587. doi: 10.1109/ICUS.2017.8278412.

Husain, I. (2021). *Electric and hybrid vehicles: design fundamentals*. CRC press.

Khan, M.A., Sayed, H.E., Malik, S., Zia, T., Khan, J., Alkaabi, N., and Ignatious, H. (2022). Level-5 autonomous driving—are we there yet? a review of research literature. *ACM Computing Surveys (CSUR)*, 55(2), 1–38.

Kim, M.s., Kim, B.j., Kim, C.i., So, M.h., Lee, G.s., and Lim, J.h. (2018). Vehicle dynamics and road slope estimation based on cascade extended kalman filter. In *2018 International Conference on Information and Communication Technology Robotics (ICT-ROBOT)*, 1–4. doi:10.1109/ICT-ROBOT.2018.8549905.

Li, J.N., Liu, X., Ru, X.F., and Xu, X. (2020). Disturbance rejection adaptive fault-tolerant constrained consensus for multi-agent systems with failures. *IEEE Transactions on Circuits and Systems II: Express Briefs*, 67(12), 3302–3306.

Liu, Y., Wei, L., Fan, Z., Wang, X., and Li, L. (2023). Road slope estimation based on acceleration adaptive interactive multiple model algorithm for commercial vehicles. *Mechanical Systems and Signal Processing*, 184, 109733.

Sun, J., Geng, Z., Lv, Y., Li, Z., and Ding, Z. (2018). Distributed adaptive consensus disturbance rejection for multi-agent systems on directed graphs. *IEEE Transactions on Control of Network Systems*, 5(1), 629–639.

Vásquez Cruz, R., Guerrero Castellanos, J., and Castellanos Velasco, E. (2024). Discrete implementation of an extended state observer for a laser beam system (lbs): Simulations and experimental results. In *2024 Memorias del Congreso Nacional de Control Automático (CNCA)*, 560–565. doi: doi.org/10.58571/CNCA.AMCA.2024.095.

Xia, G., Yan, R., Tang, X., and Sun, B. (2019). Slope shift strategy for automatic transmission vehicles based on road slope and vehicle mass identification. *International journal of vehicle design*, 81(3-4), 191–211.

Yong, W., Guan, X., Wang, B., and Ding, M. (2019). Research on the real-time identification approach of longitudinal road slope and maximum road friction coefficient. *International journal of vehicle design*, 79(1), 18–42.

Yue, H., Jing, H., Dai, Z., Lin, J., Ma, Z., Zhao, C., and Zhang, P. (2024). Optimization of shift strategy based on vehicle mass and road gradient estimation. *World Electric Vehicle Journal*, 15(12).

 https://doi.org/10.58571/CNCA.AMCA.2025.071